ORIGINAL PAPER

Ti-in-zircon thermometry: applications and limitations

Bin Fu · F. Zeb Page · Aaron J. Cavosie ·
John Fournelle · Noriko T. Kita · Jade Star Lackey ·
Simon A. Wilde · John W. Valley

Abstract The titanium concentrations of 484 zircons with U-Pb ages of ∼1 Ma to 4.4 Ga were measured by ion microprobe. Samples come from 45 different igneous rocks (365 zircons), as well as zircon megacrysts (84) from kimberlite, Early Archean detrital zircons (32), and zircon reference materials (3). Samples were chosen to represent a large range of igneous rock compositions. Most of the zircons contain less than 20 ppm Ti. Apparent temperatures

Communicated by T. L. Grove.

B. Fu · F. Z. Page · J. Fournelle · N. T. Kita · J. W. Valley (✉)
Department of Geology and Geophysics,
University of Wisconsin, Madison, WI 53706, USA
e-mail: valley@geology.wisc.edu

A. J. Cavosie
Department of Geology, University of Puerto Rico,
Mayagüez, PR 00681-9017, USA

J. S. Lackey
Geology Department, Pomona College, Claremont,
CA 91711, USA

S. A. Wilde
Department of Applied Geology, Curtin University
of Technology, Perth, WA 6845, Australia

Present Address:
B. Fu
School of Earth Sciences, The University of Melbourne,
Parkville, VIC 3010, Australia

Present Address:
F. Z. Page
Geology Department, Oberlin College, Oberlin, OH 44074, USA

for zircon crystallization were calculated using the Ti-in-zircon thermometer (Watson et al. 2006, Contrib Mineral Petrol 151:413–433) without making corrections for reduced oxide activities (e.g., TiO_2 or SiO_2), or variable pressure. Average apparent Ti-in-zircon temperatures range from 500° to 850°C, and are lower than either zircon saturation temperatures (for granitic rocks) or predicted crystallization temperatures of evolved melts (∼15% melt residue for mafic rocks). Temperatures average: 653 ± 124°C (2 standard deviations, 60 zircons) for felsic to intermediate igneous rocks, 758 ± 111°C (261 zircons) for mafic rocks, and 758 ± 98°C (84 zircons) for mantle megacrysts from kimberlite. Individually, the effects of reduced a_{TiO_2} or a_{SiO_2}, variable pressure, deviations from Henry's Law, and subsolidus Ti exchange are insufficient to explain the seemingly low temperatures for zircon crystallization in igneous rocks. MELTs calculations show that mafic magmas can evolve to hydrous melts with significantly lower crystallization temperature for the last 10–15% melt residue than that of the main rock. While some magmatic zircons surely form in such late hydrous melts, low apparent temperatures are found in zircons that are included within phenocrysts or glass showing that those zircons are not from evolved residue melts. Intracrystalline variability in Ti concentration, in excess of analytical precision, is observed for nearly all zircons that were analyzed more than once. However, there is no systematic change in Ti content from core to rim, or correlation with zoning, age, U content, Th/U ratio, or concordance in U-Pb age. Thus, it is likely that other variables, in addition to temperature and a_{TiO_2}, are important in controlling the Ti content of zircon. The Ti contents of igneous zircons from different rock types worldwide overlap significantly. However, on a more restricted regional scale, apparent Ti-in-zircon temperatures correlate with whole-rock SiO_2 and HfO_2 for plutonic rocks

of the Sierra Nevada batholith, averaging 750°C at 50 wt.% SiO_2 and 600°C at 75 wt.%. Among felsic plutons in the Sierra, peraluminous granites average 610 ± 88°C, while metaluminous rocks average 694 ± 94°C. Detrital zircons from the Jack Hills, Western Australia with ages from 4.4 to 4.0 Ga have apparent temperatures of 717 ± 108°C, which are intermediate between values for felsic rocks and those for mafic rocks. Although some mafic zircons have higher Ti content, values for Early Archean detrital zircons from a proposed granitic provenance are similar to zircons from many mafic rocks, including anorthosites from the Adirondack Mts (709 ± 76°C). Furthermore, the Jack Hills zircon apparent Ti-temperatures are significantly higher than measured values for peraluminous granites (610 ± 88°C). Thus the Ti concentration in detrital zircons and apparent Ti-in-zircon temperatures are not sufficient to independently identify parent melt composition.

Introduction

Zircon is a common accessory mineral found in diverse lithologies. The chemical substitution of a variety of elements and isotopes of geochemical interest (e.g., U, Th, Pb, Hf, REE, Ti, Li, and O) and slow intracrystalline diffusion rates (e.g., Cherniak et al. 1997a, b; Peck et al. 2003; Cherniak and Watson 2007; Page et al. 2007b; Ushikubo et al. 2008) have made zircon a staple of geochronologic, stable isotope, and trace element studies.

Watson and Harrison (2005) and Watson et al. (2006) experimentally calibrated the titanium concentration in zircon as a function of temperature of formation and the activity of TiO_2. The theoretical calculations of Harrison et al. (2005) and further experiments of Ferry and Watson (2007) suggest the substitution:

$$TiO_2 + ZrSiO_4 = ZrTiO_4 + SiO_2$$
$$rutile + zircon = Ti^{IV} - zircon + quartz \tag{1}$$
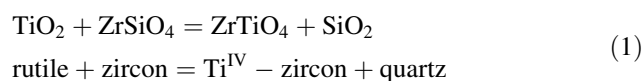
The resulting titanium-in-zircon (hereafter called Ti-in-zircon) thermometer is calibrated by analyses of both synthetic and natural zircons, which yield a precision of ± 5°C (Watson et al. 2006). This thermometer has the potential to create an invaluable link between the chronologic and geochemical information preserved in zircon, and the petrology of its host rock. The experimental calibration shows that titanium compositions in zircon are highly dependant on temperature, which suggests that the thermometer will be remarkably precise. However,

accuracy has not been independently evaluated for magmatic zircons.

Titanium-in-zircon thermometry has been applied to a growing number of natural zircons (Watson and Harrison 2005, 2006; Fu et al. 2005; Watson et al. 2006; Bea et al. 2006; Claiborne et al. 2006; Coogan and Hinton 2006; Schmitt and Vazquez 2006; Baldwin et al. 2007; Harrison et al. 2007; Page et al. 2007a; Taylor et al. 2007; Trail et al. 2007), however, many of the analyzed grains lack a petrologic context. Watson and Harrison (2005) and Harrison et al. (2007) used the Ti-in-zircon thermometer to estimate an average crystallization temperature of ~ 700°C for Early Archean detrital zircons from the Jack Hills (4.35–3.9 Ga). They interpreted these relatively low temperatures to prove that the parent magmas were wet granites, reinforcing other lines of evidence that Earth had settled into a pattern of crust formation, erosion, and sediment recycling before 4.35 Ga. These temperature estimates have not been independently verified by other means.

In this study, we apply the Ti-in-zircon thermometer to zircons from a variety of mostly plutonic, mafic to felsic igneous rocks believed to have crystallization temperatures that range from over 1,100° to below 700°C as well as detrital igneous zircons and zircon megacrysts from kimberlite. A suite of metamorphic zircons was also analyzed for comparison. For selected samples, apparent Ti-in-zircon temperatures are compared to zircon saturation temperature, solidus temperature, or modeled temperature at 85% crystallization (15% melt residue) in order to test the results on a variety of natural samples. Possible causes of differences between Ti-in-zircon temperatures and other estimates are examined, including: reduced activity of TiO_2 and SiO_2; variable pressure, fugacity of H_2O and O_2; the kinetics of Ti substitution and attainment of equilibrium; subsolidus exchange of Ti in zircon; and the fundamental question of the timing and location of zircon growth in relation to the crystallization of its igneous host.

Sample descriptions

A total of 365 zircons were analyzed from a diverse group of 45 plutonic and volcanic rocks that range from mafic to felsic in composition (Table 1). Zircons from some metagabbros contain metamorphic overgrowths and igneous cores (identified by age, trace element composition, and cathodoluminescence, CL). In addition, zircons from unknown host rocks were analyzed, including zircon megacrysts (84) from kimberlite (Page et al. 2007a), Early Archean detrital zircons (32) from the Jack Hills metaconglomerate (Wilde et al. 2001; Peck et al. 2001; Cavosie et al. 2004, 2005b, 2006, 2007), and zircon reference materials (3) (CZ3: Pidgeon et al. 1994; 91500: Wiedenbeck et al. 2004;

KIM-5: Valley et al. 1998). U-Pb ages range from <1 Ma to 4.4 Ga.

Zircons in this study span a wide range in size, morphology and CL characteristics. Multiple zircons ($\sim$10 grains) were analyzed from individual rocks to assess variability in the host rock, and some zircons were analyzed several times to assess Ti variability within a single grain. Many zircons in this study were previously analyzed for U-Pb age, oxygen isotope ratio, and trace element composition, permitting a comparison with Ti concentration.

Sample locations, host-rock types, chemical compositions, $\delta^{18}O$, and estimated zircon saturation temperatures are presented in Table 1 and Electronic supplementary material S3. A description of samples and sample locations can be found in the Appendix or, for zircons from kimberlite, in Page et al. (2007a). The major and trace element compositions of selected host rocks and zircons are also presented in Electronic supplementary material S2 to S3.

Sample preparation and analytical methods

Zircon grains were separated from their host rocks using standard density and magnetic concentration techniques. Zircons from samples of the Mid-Atlantic Ridge (Cavosie et al. 2005a) were analyzed in situ in polished rock chips. Separated zircons (or rock chips) were cast in 2.54 cm diameter epoxy cylinders, ground to their approximate mid-section and polished. Some zircon mounts in this study were prepared previously for U-Pb ion microprobe dating.

Analyses of titanium concentration in zircons (except those from the Jack Hills) were made with a CAMECA IMS-1280 ion microprobe at the University of Wisconsin, Madison. Titanium concentrations were obtained using electron multiplier pulse-counting in mono-collection mode with magnetic peak switching, a 4 nA O^- primary ion beam, 23 kV total accelerating voltage, mass resolving power (MRP) of $\sim$4,500, five cycles (15 s for $^{49}Ti^+$, 0.5 s for $^{30}Si^+$, and 3 s for $^{91}Zr^{++}$, 7–8 min total including presputtering), and $\sim$6 $\times$ 10^4 cps (counts per s) counting rate for ^{30}Si. A reduced field aperture (1,000 μm^2) was used to limit analysis to the central 5 μm^2 within a 25 μm sputtered pit. Analytical conditions and standard calibration are described in detail by Page et al. (2007a). The internal precision of a single analysis is better than 10% (2SD, 2 standard deviations) at the 5 ppm level. There is no generally available Ti standard for zircon and therefore NIST 610 glass (434 ppm Ti) was used. In order to account for matrix effects, the relative sensitivity factor of $^{49}Ti/^{30}Si$ was compared between NIST 610 and EPMA-calibrated domains in a synthetic Ti-rich zircon (800–1,500 ppm Ti, E.B. Watson). A correction factor (1.16) based on this standard was applied to SIMS data for zircons where NIST 610 was used as a standard. The working curve in a plot of $^{49}Ti/^{30}Si$ against Ti (ppm) was assumed to be linear and regressed through the origin with an accuracy of better than 8% at a low level of Ti concentrations (several to tens of ppm). Details of this calibration procedure can be found in Page et al. (2007a).

The EMPA analyses in this study were carefully evaluated to avoid secondary fluorescence that can cause erroneously high Ti contents in zircons even at distances of over 100 μm from Ti-bearing minerals (Fournelle 2008).

Titanium concentrations in Jack Hills zircons were analyzed using a CAMECA IMS-4f ion microprobe at the University of Edinburgh. Analyses were made while collecting rare earth element (REE) data. Analytical conditions were described previously (Hinton and Upton 1991; Cavosie et al. 2006), and are slightly different from the analytical methods mentioned above. A 12 nA, 10 kV O^- primary ion beam was used. A 120 volt offset was applied; the secondary ion beam was extracted at 4,380 V and MRP >500. Counting time was 20 s/cycle for ^{50}Ti with a total time of 200 s for ten cycles. Analysis of Ti using ^{50}Ti has the possibility of isobaric interference with ^{50}Cr. Analyses made of zircon standards KIM-5 and 91500 monitor instrument stability and provide a comparison of data measured on ^{50}Ti vs. ^{49}Ti. KIM-5 analyses have similar values using each method (KIM-5: 4.7 $\pm$ 1.6 (2 SD, 44 analyses, ^{49}Ti) vs. 4.0 $\pm$ 0.8 (3 analyses, ^{50}Ti)). Analyses of zircon standard 91500 are the same at the 2SD level: 4.2 $\pm$ 1.3 (7 analyses, ^{49}Ti) vs. 6.1 $\pm$ 3.0 (8 analyses, ^{50}Ti), but this standard is apparently less homogeneous in Ti and/or Cr. Coogan and Hinton (2006) recently reported that molecular interferences (including ^{50}Cr and ^{50}V) on ^{50}Ti are estimated to be <0.1 ppm, which would be negligible for most of the zircons in this study.

All average Ti contents in zircons and Ti-in-zircon temperatures in this study are reported at a level of 2 standard deviations. While many grains were analyzed in more than one spot, no coherent core-rim decrease in Ti was observed, and the data are compiled using the average for each grain in order to avoid biasing results. Averages were also compiled using all individual spot measurements and the results are not significantly different (see Table 1).

Titanium analysis locations were selected using reflected light photomicrographs, CL and back-scattered electron (BSE) images. CL and BSE were collected using a CAMECA SX51 electron microprobe at the University of Wisconsin, Madison with beam conditions of 15 kV and 10 nA. Spot analyses were correlated with U-Pb ion microprobe pits for zircons that were previously dated, including the Adirondack Mountains (McLelland et al. 2004) and Jack Hills (Cavosie et al. 2004).

Table 1 Samples from mafic to felsic igneous rocks and Ti-in-zircon temperatures (Watson et al. 2006). Zircon oxygen isotopic ratio, whole-rock SiO$_2$ content and age for most samples were taken from Valley (2003), Valley et al. (2005), and references therein (see Appendix)

Sample no.	Lithology	Location	SiO$_2$ (wt.%)	δ^{18}O, Zrc (‰)	Age (Ma)	Ti (ppm) $\pm$ 2 SD (# analyses)	Ave T, Ti-Zrc (°C, $\pm$2 SD) (# analyses)	Ave T, Ti-Zrc (°C, $\pm$2 SD) (# zircon grains)
Mafic rocks								
NC-8924A	Anorthosite	Paul Island, Nain Anorthosite Complex, Labrador		5.05	1,319	21.8 $\pm$ 18.7 (7)	808 $\pm$ 84 (7)	799 $\pm$ 76 (6)
EC90-177	Anorthosite	Koliktalik, Nain Anorthosite Complex, Labrador		6.06	1,305	10.2 $\pm$ 19.1 (7)	721 $\pm$ 139 (7)	737 $\pm$ 157 (5)
HMB93-17	Anorthosite	Kikkertavak Island, Nain Anorthosite Complex, Labrador		5.94	1,311	22.0 $\pm$ 21.9 (7)	807 $\pm$ 101 (7)	815 $\pm$ 96 (6)
HMB93-14A	Leuconorite	Tabor Island, Nain Anorthosite Complex, Labrador		6.20	1,311	15.8 $\pm$ 12.6 (5)	777 $\pm$ 78 (5)	778 $\pm$ 52 (4)
(BMH-) 01E1	Anorthosite	Woolen Mill, northeastern Marcy massif, Central Adirondack Highlands		8.82	1,155	10.8 $\pm$ 10.6 (15)	740 $\pm$ 87 (15)	737 $\pm$ 80 (11)
(BMH-) 01E2	Anorthosite	Woolen Mill, northeastern Marcy massif, Central Adirondack Highlands		8.87	1,155	8.5 $\pm$ 9.2 (24)	719 $\pm$ 79 (24)	713 $\pm$ 78 (16)
(BMH-) 01E4	Anorthosite	Woolen Mill, northeastern Marcy massif, Central Adirondack Highlands		8.84	1,155	8.6 $\pm$ 6.9 (11)	722 $\pm$ 73 (11)	720 $\pm$ 76 (10)
ODP 153-920B-2R-1, 44-50	Serpentinite	Mid-Atlantic Ridge near the Kane Transform (MARK area)			<1	27.4 $\pm$ 19.7 (8)	834 $\pm$ 71 (8)	828 $\pm$ 61 (7)
ODP 153-920B-5R-1, 59-64	Serpentinite	Mid-Atlantic Ridge near the Kane Transform (MARK area)			<1	25.3 $\pm$ 9.2 (3)	829 $\pm$ 37 (3)	829 $\pm$ 37 (3)
ODP 153-922B-2R-2, 20-23(a, b)	Gabbro	Mid-Atlantic Ridge near the Kane Transform (MARK area)			<1	30.2 $\pm$ 8.6 (14)	848 $\pm$ 31 (14)	848 $\pm$ 31 (14)
OM-473	Monzogabbro	Palermo, Serra do Mar Alkaline-Peralkaline Suite	53.22	5.52	584	6.8 $\pm$ 2.4 (10)	707 $\pm$ 29 (10)	707 $\pm$ 29 (10)
DD78-17	Gabbro	Sturgeon Lake, Pike Lake gabbro, Wabigoon Subprovince	53.30	5.08	2,739	11.4 $\pm$ 6.1 (10)	750 $\pm$ 44 (10)	750 $\pm$ 44 (10)
DD78-19	Gabbro Pegmatite	Kakagi Lake, Wabigoon Subprovince		4.88	2,723	12.3 $\pm$ 8.8 (10)	756 $\pm$ 60 (10)	756 $\pm$ 60 (10)
I14	Gabbro	Ivanhoe Quadrangle, Sierra Nevada		5.47	110	4.7 (1)	679 (1)	679 (1)
CM20	Gabbro	Colvin Mountain, Sierra Nevada		5.64	120	10.4 $\pm$ 8.2 (9)	739 $\pm$ 72 (9)	733 $\pm$ 72 (8)
WR9	Norite	Near Cuidado Mountain (White River Quadrangle), Sierra Nevada		6.76	115	11.1 $\pm$ 6.5 (8)	747 $\pm$ 54 (8)	745 $\pm$ 62 (6)
3S48	Diorite	Mud Lakes, Dinkey Creek Pendant, Sierra Nevada Batholith	52.04	7.54	90	7.1 $\pm$ 5.2 (13)	707 $\pm$ 64 (13)	711 $\pm$ 48 (10)
TEMORA-1	Gabbroic Diorite	Middledale, Lachlan Fold Belt, New South Wales, Australia	47.84	7.93	417	12.1 $\pm$ 4.8 (10)	757 $\pm$ 34 (10)	757 $\pm$ 36 (9)

Table 1 continued

Sample no.	Lithology	Location	SiO$_2$ (wt.%)	δ ^{18}O, Zrc (‰)	Age (Ma)	Ti (ppm) $\pm$ 2 SD (# analyses)	Ave T, Ti-Zrc (°C, $\pm$2 SD) (# analyses)	Ave T, Ti-Zrc (°C, $\pm$2 SD) (# zircon grains)
TEMORA-2	Gabbroic Diorite	Middledale, Lachlan Fold Belt, New South Wales, Australia	49.45	8.20	417	10.2 $\pm$ 7.3 (16)	738 $\pm$ 65 (16)	737 $\pm$ 69 (14)
(BMH-) 01E3	Metaferrogabbro	Woolen Mill, northeastern Marcy massif, Central Adirondack Highlands	43.25	8.84	1,155	7.7 $\pm$ 7.2 (19)	714 $\pm$ 61 (19)	711 $\pm$ 52 (10)
JH79-191	Metagabbro	Mount Stuart batholith, Big Jim Mountain, Washington		7.54	96	21.2 $\pm$ 8.1 (10)	810 $\pm$ 43 (10)	810 $\pm$ 43 (10)
PCS-1	Metagabbro	Metagabbro sill at Prairie Creek, Central Black Hills, South Dakota			1,883	22.0 $\pm$ 42.7 (10)	790 $\pm$ 160 (10)	786 $\pm$ 160 (9)
BJS-1	Metagabbro	Metagabbro sill at Bogus Jim Creek, Central Black Hills, South Dakota			1,974	13.3 $\pm$ 11.5 (10)	760 $\pm$ 85 (10)	758 $\pm$ 88 (9)
SC1/2	Felsic Segregation in Gabbro	Cuillins outer Eucrite Serices, Isle of Skye, Scotland		2.50	58	22.7 $\pm$ 11.6 (14)	816 $\pm$ 54 (14)	816 $\pm$ 54 (14)
SR314	Feldspathic Peridotite	Layered mafic/ultramafic complex, Isle of Rum, Scotland			60	17.6 $\pm$ 12.1 (11)	789 $\pm$ 71 (11)	789 $\pm$ 71 (11)
J2-12 [No. 39]	Trondhjemite Pod in Gabbro	Preston Gabbro, Griswold, Connecticut		6.35	424	10.2 $\pm$ 17.3 (11)	728 $\pm$ 107 (11)	723 $\pm$ 66 (10)
DB-3	Granophyric Phase in Gabbro	Crossport "C" sill, Eastport, Idaho		4.94	1,433	9.1 $\pm$ 12.9 (10)	717 $\pm$ 117 (10)	717 $\pm$ 117 (10)
DB-10	Granophyric Phase in Gabbro	Crossport "C" sill, Eastport, Idaho		4.90	1,433	7.8 $\pm$ 6.7 (11)	713 $\pm$ 78 (11)	711 $\pm$ 80 (10)
NS-1	Granophyric Phase in Metagabbro	Metagabbro sill at Blue Draw, Nemo, Black Hills, South Dakota			2,170	16.3 $\pm$ 11.9 (9)	781 $\pm$ 67 (9)	783 $\pm$ 69 (8)
All mafic rocks above, average						13.7 $\pm$ 18.3 (304)	755 $\pm$ 112 (304)	758 $\pm$ 111 (261)
Felsic-intermediate rocks								
	Metaluminous							
W21	Tonalite	Pine Flat Road, Near Cuidado Mountain (White River Quadrangle), Sierra Nevada Batholith		7.04	100	8.9 $\pm$ 8.3 (10)	724 $\pm$ 85 (10)	723 $\pm$ 70 (7)
1S108	Tonalite	Glen Aulin Tonalite, East of May Lake, Sierra Nevada Batholith	57.64	6.35	93.1	12.2 $\pm$ 8.5 (10)	751 $\pm$ 93 (10)	751 $\pm$ 73 (5)
1S91	Tonalite	Bass Lake Tonalite, North Fork, Sierra Nevada Batholith	67.16	7.30	114	4.1 $\pm$ 3.2 (16)	662 $\pm$ 63 (16)	662 $\pm$ 34 (7)
1S40	Tonalite	Bass Lake Tonalite, West of Prather, Sierra Nevada Batholith	63.36	7.91	114	2.8 $\pm$ 2.0 (13)	636 $\pm$ 55 (13)	638 $\pm$ 37 (6)
1S88	Granodiorite	Lamark Granodiorite, South Shore of Lake Edison, Sierra Nevada Batholith	62.31	5.84	92	6.9 $\pm$ 5.1 (14)	705 $\pm$ 61 (14)	704 $\pm$ 39 (6)
	Peraluminous							

Table 1 continued

Sample no.	Lithology	Location	SiO$_2$ (wt.%)	δ^{18}O, Zrc (‰)	Age (Ma)	Ti (ppm) $\pm$ 2 SD (# analyses)	Ave T, Ti-Zrc (°C, $\pm$2 SD) (# analyses)	Ave T, Ti-Zrc (°C, $\pm$2 SD) (# zircon grains)
1S2	Granodiorite	Tharps Peak Pluton, Lake Kaweah, Sierra Nevada Batholith	73.50	7.64	110	3.2 $\pm$ 6.7 (20)	623 $\pm$ 132 (20)	623 $\pm$ 96 (7)
1S79	Granite	Dinkey Dome Pluton, West Side of Dinkey Dome, Sierra Nevada Batholith	73.40	7.67	90	1.4 $\pm$ 1.0 (11)	592 $\pm$ 41 (11)	593 $\pm$ 33 (5)
1S77	Granite	Dinkey Dome Pluton, East Side of Dinkey Dome, Sierra Nevada Batholith	76.90	7.63	90	1.7 $\pm$ 1.6 (11)	601 $\pm$ 56 (11)	599 $\pm$ 42 (5)
1S51	Granite	Dinkey Dome Pluton, East Side of Dinkey Dome, Sierra Nevada Batholith	76.70	7.76	90	4.6 $\pm$ 11.2 (14)	644 $\pm$ 151 (14)	638 $\pm$ 127 (6)
1S58	Granite	Dinkey Dome Pluton, West Side of Dinkey Dome, Sierra Nevada Batholith	75.00	7.77	90	1.8 $\pm$ 4.6 (11)	588 $\pm$ 116 (11)	591 $\pm$ 80 (6)
All felsic rocks above, average						4.5 $\pm$ 8.5 (130)	651 $\pm$ 136 (130)	653 $\pm$ 124 (60)
Volcanic rocks								
Zircon #50 (Acw R30)	Basanite	Chantaburi, Thailand				1.8 $\pm$ 0.4 (7)	608 $\pm$ 16 (7)	608 $\pm$ 7 (6)
HRT C1 2R (HRT-C)	Rhyolite	Huckleberry Ridge Tuff (Member C), Yellowstone	75.60	5.57	2.1	7.2 $\pm$ 3.8 (10)	710 $\pm$ 47 (10)	710 $\pm$ 47 (10)
HRT-3a	Rhyolite	Huckleberry Ridge Tuff, Yellowstone	77.30		2.1	19.5 $\pm$ 32.8 (10)	780 $\pm$ 155 (10)	786 $\pm$ 155 (9)
MFT-2	Rhyolite	Mesa Falls Tuff, Yellowstone	77.60	3.62	1.3	28.6 $\pm$ 59.3 (10)	804 $\pm$ 208 (10)	787 $\pm$ 206 (8)
LCT-2B	Rhyolite	Lava Creek Tuff, Yellowstone	73.80		0.6	3.0 $\pm$ 1.1 (10)	644 $\pm$ 28 (10)	645 $\pm$ 26 (9)
Pegmatite								
00W35	Pegmatite in skarn	Willsboro, Central Adirondack Highlands, NY		0.96	900	0.3 $\pm$ 0.2 (5)	500 $\pm$ 32 (5)	498 $\pm$ 25 (2)
Detrital zircons								
01JH36	Quartzite	Jack Hills, Western Australia		4.6–5.3	>4,000	15.3 $\pm$ 15.1 (3)	772 $\pm$ 101 (3)	774 $\pm$ 14 (2)
01JH54	Conglomerate	Jack Hills, Western Australia		5.3–7.3	>4,000	11.1 $\pm$ 17.0 (20)	733 $\pm$ 120 (20)	733 $\pm$ 95 (12)
01JH60	Conglomerate	Jack Hills, Western Australia		6.0–6.7	>4,000	5.9 $\pm$ 6.6 (4)	689 $\pm$ 81 (4)	689 $\pm$ 81 (4)
W74/2	Conglomerate	Jack Hills, Western Australia		5.3–5.4	>4,000	14.1 $\pm$ 27.4 (13)	743 $\pm$ 162 (13)	740 $\pm$ 127 (2)
W74/3	Conglomerate	Jack Hills, Western Australia		4.6–7.3	>4,000	7.1 $\pm$ 14.0 (15)	695 $\pm$ 109 (15)	695 $\pm$ 116 (12)
Total number of analyses/grains						(541)	(541)	(397)
Standards								
KIM-5	Megacryst in Kimberlite	Kimberley, South Africa		5.09	92[a]	4.7 $\pm$ 1.6 (48)	678 $\pm$ 22 (48)	678 (1)
91500	Zircon crystal	Kuehl Lake, Ontario, Canada		9.94	1,065	5.2 $\pm$ 3.0 (15)	684 $\pm$ 42 (15)	684 (1)
CZ-3	Zircon crystal	Detrital grain from Sri Lanka			564	4.8 $\pm$ 1.6 (2)	680 $\pm$ 26 (2)	680 (1)

[a] Cavosie et al. (2005). Abbreviations: *Zrc* zircon, *n* number of spots or crystals, *SD* standard deviation

Results

Titanium concentrations for all samples are plotted in Fig. 1, tabulated in the Electronic supplementary material S1, and summarized in Table 1. Data for kimberlite zircons are reported in Page et al. (2007a). Most of the zircons in this study (~90%) have Ti concentrations of less than 20 ppm, including all zircons from felsic and intermediate plutonic rocks and the majority of zircons from mafic samples (Fig. 1). Some of the highest Ti abundances were found in gabbro and gabbroic dikes in serpentinite (17–48 ppm) from the Mid-Atlantic Ridge, and 12 of the 84 analyzed mantle zircon megacrysts from kimberlite have Ti concentration from 20 to 53 ppm (Page et al. 2007a). Ti-in-zircon temperatures were estimated using the calibration of Watson et al. (2006), assuming unit activities of TiO_2 and SiO_2 and applying no pressure correction. The effects of applying these corrections are discussed below. The average Ti-in-zircon temperatures for individual rock samples are listed in Table 1 and range from ~500° to ~850°C.

Titanium in zircon from different rock types

In general, Ti concentration in zircon appears to decrease from mafic to felsic rocks, which translates to decreasing Ti-in-zircon temperatures (Figs. 1, 2). The Ti-in-zircon temperatures for the central Sierra Nevada batholith are compared with the SiO_2 content of the host rock in Fig. 3 and Table 1. Average temperatures decrease by ~100°C from gabbro/norite/diorite (725 ± 66°C, 25 zircons) through tonalite (691 ± 104°C, 25 zircons) to granodiorite/granite (626 ± 108°C, 35 zircons). Likewise Ti-in-zircon temperatures for the Sierran zircons correlate inversely to HfO_2 in zircon (Fig. 4; Electronic supplementary material S2).

Ti-in-zircon temperatures for megacrysts in kimberlite are identical to those in zircons from mafic rocks (Fig. 2). In contrast to plutonic rocks, the Ti contents of zircons from different rhyolites of the main Yellowstone eruptive phases are more variable and record average temperatures ranging from 645 ± 26°C to 787 ± 206°C.

Early Archean detrital zircons

In addition to zircons separated from igneous rocks, Early Archean detrital zircons (4.4–3.9 Ga, Wilde et al. 2001; Peck et al. 2001; Cavosie et al. 2004, 2005b, 2006) were also analyzed. Well-preserved igneous zircons (or domains within zircons) identified by REEs, age concordance, $\delta^{18}O$, and CL image were selected for Ti analysis based on the classification (type 1) of Cavosie et al. (2006). Zircon domains that are hydrothermally altered or radiation-damaged with anomalous REE chemistry or ion microprobe U-Pb age discordance (type 2, Cavosie et al. 2006) are not considered primary, and were not analyzed for Ti. Early Archean zircons from the Jack Hills were found to contain an average of 9.5 ± 15.4 ppm Ti (55 analyses) yielding $T = 717 ± 104°C$ (32 zircons).

### Ti variability within single zircon grains

Variability in Ti within individual zircons in excess of analytical precision is observed in nearly all zircons that were analyzed in more than one spot. Converted into Ti-in-zircon temperature, a comparison of Ti concentrations in zircon cores vs. rims (identified in CL and BSE images) shows no consistent pattern (Fig. 5). We do not observe a consistent decrease in Ti concentration in zircon from core to rim as might be expected (Watson and Harrison 2005) for growth zoning in igneous zircon during cooling although more complex thermal models could be constructed to explain this variability. Titanium-in-zircon temperatures similarly show no systematic change with regard to U content, Th/U ratio, or U-Pb age or concordance for non-metamict grains.

Recent studies have shown that Ti correlates with Y, Ce and P as well as CL zonation in some zircon grains at a nano- to micro-meter scale (Holden et al. 2005; Hofmann et al. 2007). This zonation is interpreted to reflect variable Ti substitution within zircon and is clearly distinct from the secondary Ti-rich phases that are reported within late cracks in other zircons (Harrison and Schmidt 2007). Late crack-filling phases were avoided in this study by careful imaging, before and after ion microprobe analysis, but occasional Ti-rich inclusions may still explain high Ti outliers.

Zircons from the Woolen Mill metagabbro and meta-anorthosite from the Adirondack Mountains contain igneous cores and granulite-facies overgrowth rims distinguishable by CL and U-Pb age (Fig. 6; McLelland et al. 2004). Titanium concentrations in zircons from both rocks range from 4 to 21 ppm (8 ± 4 ppm, 19 zircons). In most grains, the difference in Ti content between core and rim is less than 4 ppm and there is no consistent gradient in composition (Fig. 5). Both igneous cores (715 ± 40°C) and metamorphic overgrowths (720 ± 18°C) yield essentially the same temperature (Fig. 6).

Inherited zircons are generally interpreted as evidence that the host magma was saturated in zircon. One may argue that zircon inheritance accounts for the Ti variability within single zircon grains and/or Ti outliers within single rock samples, and this might be the case for

Fig. 1 Titanium concentrations in zircons from mafic and felsic igneous rocks shown as individual measurements and their respective Ti-in-zircon temperatures calculated assuming $a_{TiO_2} = 1$ and $a_{SiO_2} = 1$ (Watson and Harrison 2005). Zircon megacrysts in kimberlite are from Page et al. (2007a). A majority of samples have average compositions less than 20 ppm (~800°C), *vertical dotted line*. The number of rock samples in each suite follows the suite name *in parentheses*
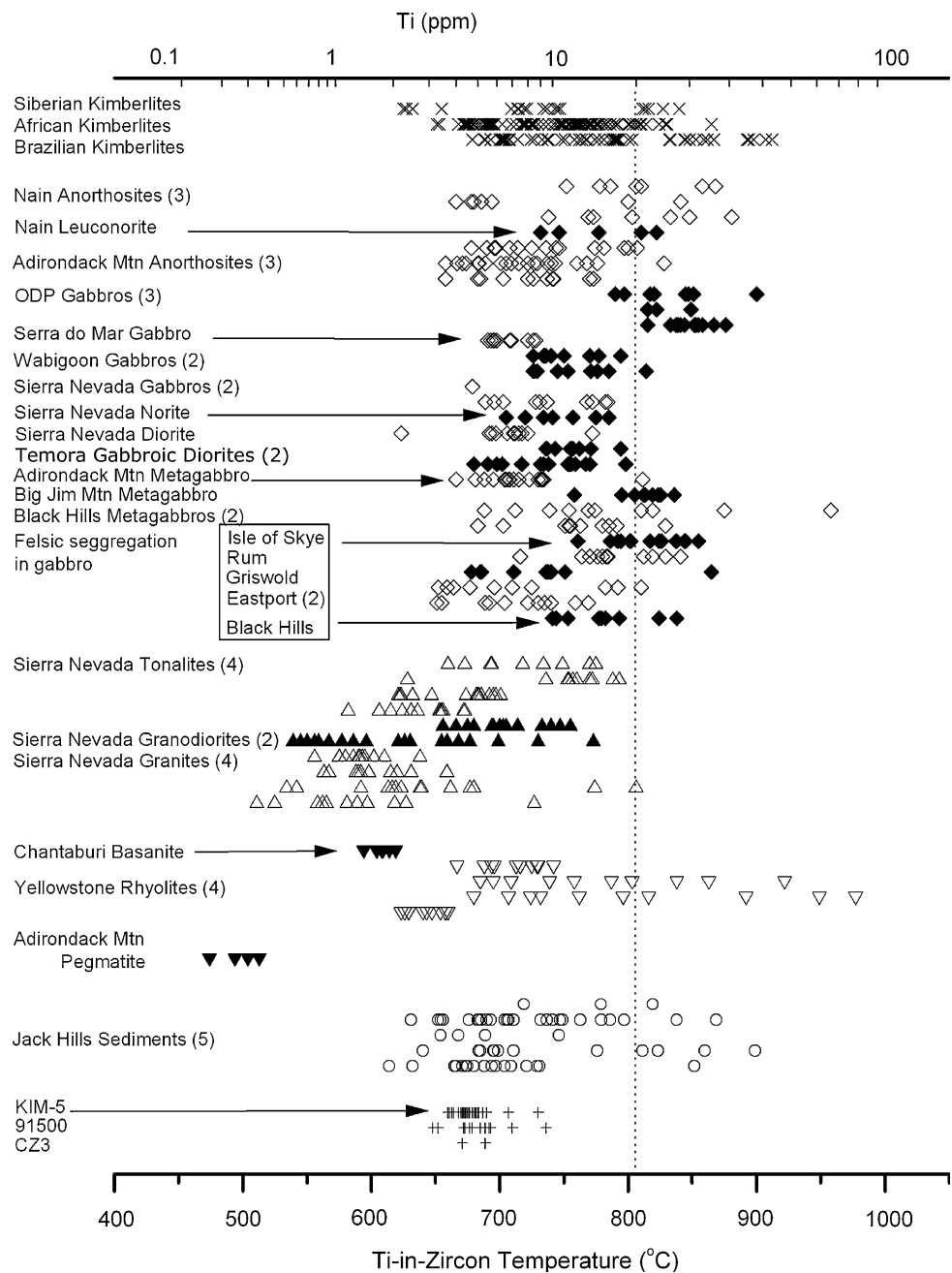
some of the zircon grains analyzed in felsic rocks. It must be pointed out, however, that all the analyzed zircons in the present study were carefully selected based on CL and/or BSE images and that multiple analyses for many zircons in the felsic rocks were performed. Our results indicate that most Ti-in-zircon temperatures are lower than zircon saturation temperatures (see "Discussion"). By contrast, zircons in most mafic rocks display homogeneous CL-zonation, and there is only one Ti population. Therefore, the effect of zircon inheritance appears to be minor.

Discussion

The analytical precision of Ti-in-zircon temperatures is excellent, but the accuracy of these estimates has not been independently evaluated for magmatic zircons. Do these values accurately record the crystallization temperature of each growth zone in a zircon such that inter- and intra-crystalline variability represents actual physical processes including temperature variation during growth, or magma convection or mixing? Alternatively, are there other factors that influence the substitution of Ti into zircon? Possible

factors include: variation of TiO_2 or SiO_2 activity, a pressure correction, resetting of Ti concentration by subsolidus alteration or diffusion, or accuracy of the thermometer calibration. It is also possible that some igneous zircons grow in evolved hydrous magmas at lower temperatures than the solidus of the bulk rock that hosts them, that the incorporation of Ti into the zircon structure is not an equilibrium process, or that Ti substitution violates Henry's Law due to structural defects, variable fO_2, or other trace-element effects that are not duplicated in the experiments. These factors are discussed below.

Crystallization temperature of melt

The Ti content of zircons from igneous rocks generally decreases from mafic (13.7 ± 18.3 ppm, 304 analyses) to felsic (4.5 ± 8.5 ppm, 130 analyses) compositions, but with broad overlap (Fig. 1). These compositions yield a range of average Ti-in-zircon temperatures: 591 ± 80°C (sample 1S58) to 751 ± 73°C (1S108) for felsic to intermediate igneous rocks, and 697°C (I14) to 848 ± 31°C

Fig. 3 Plot of Ti-in-zircon (Zrc) temperature (average value of different zircon grains for each rock sample) against whole-rock (WR) SiO_2 (wt.%) for mafic to felsic plutonic rocks from the Sierra Nevada batholith. Sierran samples define a trend in which Ti-in-zircon temperature decreases with increasing SiO_2, however, maximum temperatures are only ~750°C

Fig. 2 Histograms of Ti-in-zircon temperatures for kimberlites, mafic rocks, and intermediate and felsic igneous rocks (see Table 1). Abbreviations in parentheses: *SD* standard deviation, *n* number of zircon grains analyzed
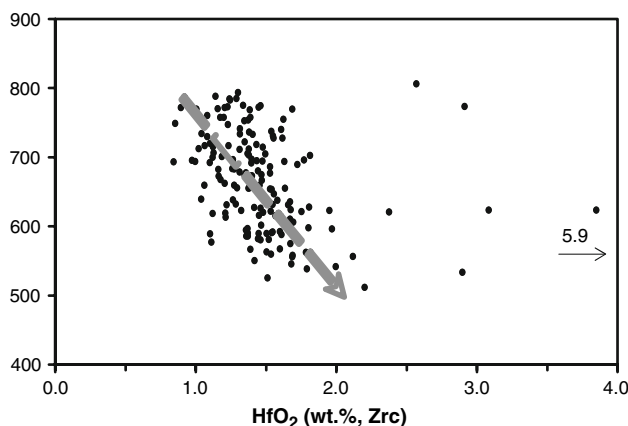
Fig. 4 Plot of Ti-in-zircon temperature against HfO_2 in zircons from the Sierra Nevada batholith showing a slight negative correlation (HfO_2 <2 wt.%). Zrc:zircon

(ODP 153-922B-2R-2, 20–23) for mafic rocks (Fig. 2, Table 1). Temperatures obtained in this study are consistent with most of the smaller dataset (37 analyses) of natural zircons in Watson et al. (2006) (but see the Labait harzburgite, Ferry and Watson 2007).

While temperatures of crystallization are difficult to accurately constrain due to uncertainties, including pressure, water activity, and the actual rock compositions at the time of zircon growth, it is possible to broadly estimate the conditions of zircon crystallization. Zircons in a cooling magma grow over a range of temperature that begins at

zircon saturation and culminates at the solidus (see Harrison et al. 2007, for problems in calculating zircon saturation temperatures). Even in simplified systems (e.g., $NaAlSi_3O_8$-$CaAl_2Si_2O_8$), there is an interval of some 100° to 200°C between the solidus and the liquidus for most compositions. Measurements on erupting lavas show that rhyolitic to basaltic magmas reach the surface at temperatures typically between 800° and 1,200°C (Carmichael et al. 1974) and likely crystallization temperatures of felsic to mafic plutonic rocks vary from ~600° to 1,100°C, respectively.

To quantitatively estimate crystallization temperature, the MELTs algorithm (Ghiorso et al. 1995; Asimow and Ghiorso 1998) was employed based on the assumption that the whole-rock chemical composition should represent initial melt chemical composition (Electronic supplementary material S3, S4). Liquidus temperature estimated by MELTs varies from ~1,200–900°C, largely dependent on wt.% SiO_2 and water activity. For granitic rocks (e.g., from Yellowstone or the Sierra Nevada batholith), no solidus temperature could be calculated at water contents of 0.2–4 wt.%. At 1–4 wt.% H_2O, the MELTs program either could not give a reasonable liquidus temperature or the calculation failed at less than 85% crystallization (>15% melt residue). At 15% melt residue, temperatures for some mafic rocks in our study, if wet (4 wt.% H_2O), are 100°–200°C lower than if dry (0.2 wt.% H_2O).
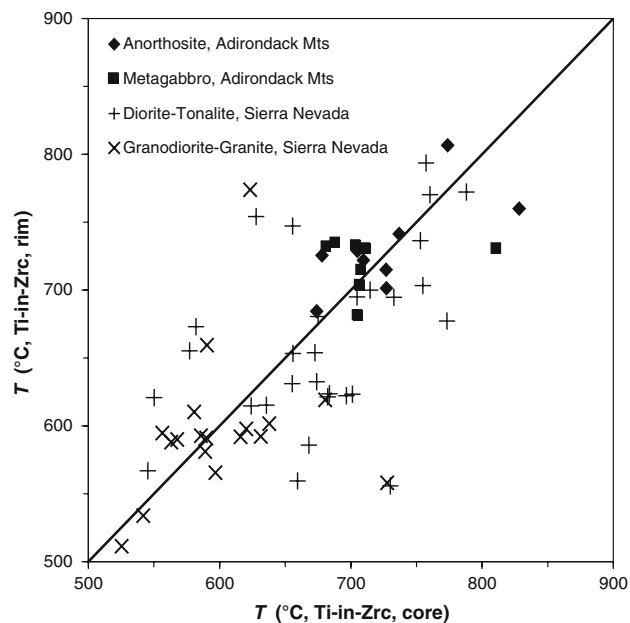

Fig. 5 Comparison of Ti-in-zircon temperatures, rim vs. core, within single zircon crystals from the Adirondack Mountains and Sierra Nevada batholith. For metagabbro, cores are igneous and rims are metamorphic. All other zircons are judged to be magmatic based on CL image and composition

The average Ti-in-zircon temperatures obtained in this study (710° to 750°C) are lower than the calculated crystallization temperatures of melts (>15% melt residue). In comparison to these broad estimates, the Ti compositions of many igneous zircons yield surprisingly low temperatures and thus may record a late crystallization history of evolved melts. These Ti-in-zircon temperatures could be comparable to solidus temperatures only if the zircons formed during crystallization of the last 15% melts.

TiO_2 and SiO_2 activity

The activity of both TiO_2 and SiO_2 must be known to accurately apply the Ti-in-zircon thermometer. However, if Ti substitutes for Si^{IV} in zircon (Eq. 1), then undersaturation with respect to silica would result in an overestimate of temperature (Page et al. 2007a; Ferry and Watson 2007), which fails to explain the generally low temperature estimates reported here for a wide variety of host-rock compositions. It should be pointed out that many host rocks in this study contain quartz. Furthermore, most silicic melts have an activity of SiO_2, $a_{SiO_2} \geq 0.3$ ($T = 600$–$1,200$°C; Carmichael et al. 1970). In contrast, undersaturation with respect to rutile would result in temperature estimates that are erroneously low. Since rutile is not reported in most of the rocks studied, estimates of the activity of TiO_2 will be discussed further. The presence of Ti-rich minerals such as ilmenite or titanite in igneous rocks may suggest a relatively high TiO_2 activity at the time of zircon crystallization, assuming that the Ti-phase and zircon crystallized together. However, even ilmenite-bearing rocks (Bishop Tuff) have been found to have a_{TiO_2} as low as 0.6 (Watson et al. 2006). Furthermore, it is possible that an apparently coexisting Ti-rich mineral was not in equilibrium with zircon at the time of crystallization. Alternatively, analysis of Ti in coexisting quartz has been used to estimate a_{TiO_2} (Watson et al. 2006; Wark and Watson 2006). Experimental results indicate that rutile activity in magma is not strongly dependent on P_{total} or water content but is controlled by temperature (Ryerson and Watson 1987; Hayden and Watson 2007). Watson and Harrison (2005) suggested that most natural melts capable of crystallizing zircons (i.e., saturated in $ZrSiO_4$) have TiO_2 activities exceeding ~0.5. Hayden and Watson (2007) show that if other variables are held constant, mafic melts will have lower a_{TiO_2} than felsic melts.

The majority of the host rocks investigated in this study contain ilmenite or titanite and some contain rutile. In certain cases (e.g., kimberlite megacrysts, detrital zircons), TiO_2 activity cannot be estimated because of the absence of coexisting phases (Ti minerals, host-rock, or quartz). However, assuming that most zircon-bearing magmas have

Fig. 6 Cathodoluminescence images of zircons from the Woolen Mill metagabbro (Adirondack Mountains). Spot analyses of Ti-in-zircon temperatures are shown (*squares*) with U-Pb ages (*ellipses* ±2 SD) (McLelland et al. 2004). Bright granulite-facies metamorphic rims have nearly identical Ti-in-zircon temperatures (∼700°C) to dark, oscillatory-zoned igneous cores that formed at higher magmatic temperatures. *Scale bars* 50 μm
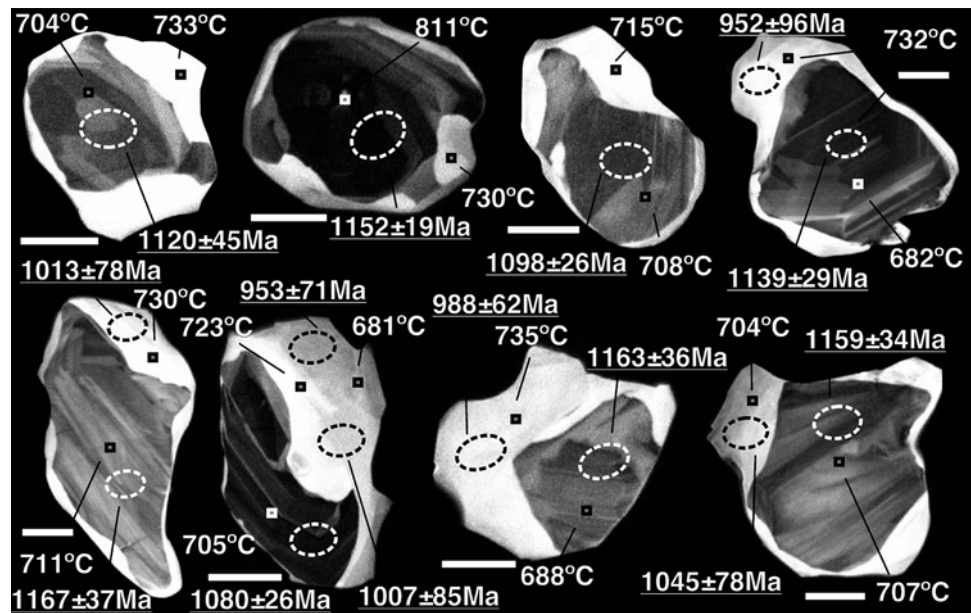
TiO$_2$ activity >0.5, it is estimated that the Ti-in-zircon thermometer underestimates temperatures by at most 70°C if a_{TiO_2} is unknown (Hayden and Watson 2007; Ferry and Watson 2007).

Pressure

Zircon synthesis experiments, upon which the calibration of the Ti-in-zircon thermometer is based, were performed at 10 kbar and taken to be representative of crustal pressure (Watson et al. 2006). In order to assess a potential pressure effect, Watson et al. (2006) performed two additional experiments at 20 kbar. Data from these experiments lie along the same calibration line as the 10 kbar runs, and the pressure effect on this thermometer was deemed to be negligible. However, the ΔV_r for Eq. (1) suggests that the pressure correction is significant, especially for the high pressures of eclogite facies and mantle rocks, and that pressures greater than 10 kbar will lead to underestimation of temperature using the current calibration (Page et al. 2007a). At a higher pressure, less Ti can substitute in zircon. The experiments of Ferry and Watson (2007) indicate a pressure correction of ∼5°C/kbar at 750°C. While this effect could be significant for zircons that formed at high pressures, it is likely to be small for most middle to lower crustal rocks. Conversely, zircons that formed in the shallow crust will likely incorporate more Ti than would be predicted by the present calibration, yielding higher temperatures. However, Ti thermometry for zircons from *all* depths (shallow crust, deep crust, mantle) in this study appears to underestimate temperatures. While a pressure

correction may be important, pressure alone cannot be responsible for low temperature estimates.

Subsolidus exchange

Meaningful application of the Ti-in-zircon thermometer to rocks with long or complex histories requires that magmatic compositions in zircon be preserved through subsequent events, such as slow cooling, alteration, or high-grade metamorphism. For instance, igneous cores of zircons must retain magmatic Ti compositions even if partly dissolved and surrounded by granulite facies zircon overgrowths. Zircons in the Adirondack Mountains (USA) provide excellent examples to test this application. In the Adirondacks, anorthosite and gabbro have experienced granulite facies metamorphism at 700–800°C (Bohlen et al. 1985), but pre-metamorphic magmatic temperatures are estimated at 1,000–1,100°C by reintegration of coexisting ophitic pyroxenes (Bohlen and Essene 1978). The Ti-in-zircon temperatures do not record this well documented history. Magmatic zircon cores (oscillatory zoned in CL and igneous ages by SHRIMP, McLelland et al. 2004) record temperatures of 700–750°C, identical within uncertainty to the temperatures of metamorphic overgrowths (Fig. 6). These igneous cores are over 250° below the initial magmatic conditions recorded by pyroxenes. There are two possible explanations: (1) the similar temperatures of core and rim could be explained if Ti exchanged during metamorphism; however, the likely slow diffusion of Ti in zircon (Watson et al. 2006; Cherniak and Watson 2007) suggests a closure temperature above 900°C.
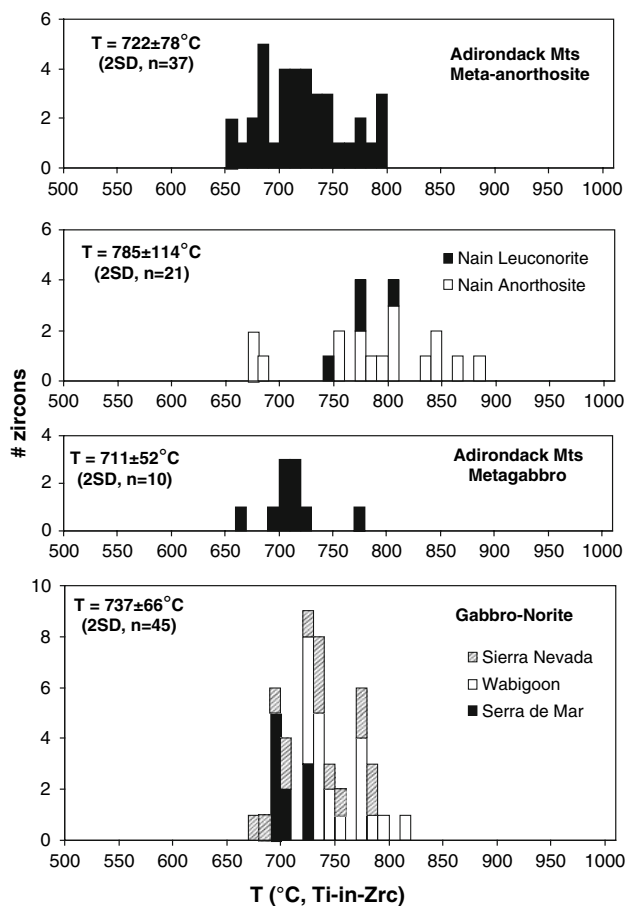
Fig. 7 Histograms of Ti-in-zircon temperatures estimated for both metamorphosed and unmetamorphosed anorthosites (Nain, Adirondacks) and gabbros (Adirondacks, Sierra Nevada, Wabigoon, Serra de Mar)
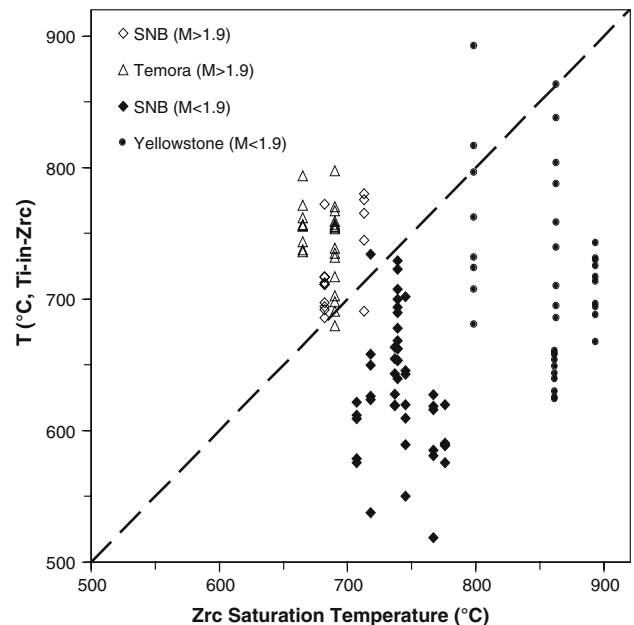

Fig. 8 Comparison of Ti-in-zircon temperatures with zircon saturation temperatures (Watson and Harrison 1983). Whole-rock chemical compositions fall both in the range of experimental calibration (*M* <1.9 *filled symbols*) and outside the recommended range (*M* > 1.9 *open symbols*, *M* = ((Na + K + 2Ca)/(Al·Si)). Sample sources: *SNB* Sierra Nevada batholith, *Temora* Temora gabbroic diorite, and *Yellowstone* Yellowstone rhyolite

(2) Ti in igneous zircon cores could lead to an underestimate of the crystallization temperatures of the bulk host rock. An obvious test of this question is to analyze zircons from similar igneous rocks elsewhere that have not experienced high-grade regional metamorphism.

Igneous zircons from a variety of unmetamorphosed gabbros were analyzed to test if metamorphosed and unmetamorphosed rocks show a systematic difference in Ti-in-zircon temperatures. Zircons from the Sierra Nevada, Wabigoon, Sierra del Mar (Fig. 7) yield nearly identical temperatures (737 ± 66°C, 45 zircons) to the igneous zircon cores from Adirondack Mountains metagabbro (711 ± 52°C, 10 zircons) or Adirondack Mountains metaanorthosite (722 ± 78°C, 37 zircons). Anorthosite/leuconorite from the Nain Plutonic Suite did not experience any prolonged regional metamorphism (Hamilton et al. 1994) and zircons from this unmetamorphosed anorthosite yield only slightly higher temperatures (785 ± 114°C, 21 zircons) than meta-anorthosite (Adirondacks Mountains, Fig. 7). The results from zircons from unmetamorphosed

gabbros show that low temperatures recorded by igneous zircon cores from Adirondack mafic rocks are not uniquely the result of high grade regional metamorphism. Thus, there is no evidence that zircon compositions from unmetamorphosed gabbros are reset.

Zircon saturation temperature and late crystallization in evolved melts

The equilibrium growth of zircon in a cooling magma begins at the temperature that zircon first becomes saturated and ends at the solidus. Thus, Ti-in-zircon thermometry of zircons from simple magmatic systems should record the zircon saturation temperature in zircon cores, with decreasing temperatures towards the rim. Zircon saturation temperatures can be estimated (Watson and Harrison 1983; Baker et al. 2002; Hanchar and Watson 2003) and predict the saturation of zircon as a function of bulk-rock composition and temperature (but see Harrison et al. 2007). Saturation temperatures for a subset of rocks in this study were estimated using the experimental calibration of Watson and Harrison (1983) (compositional range: $M = (Na + K + 2\,Ca)/(Al \cdot Si) = 0.9$–1.9). The results are listed in the Electronic supplementary material S3 and illustrated in Fig. 8. Saturation temperatures are calculated

assuming that whole rock data reflect magma compositions without correction for possible phenocrysts or xenocrysts. The enjoinder that only actual melt compositions should be used (Harrison et al. 2007) makes accurate saturation thermometry impractical for most rocks, but trends in the data may still have qualitative significance. Clemens (2003) pointed out that zircon and zirconium behavior is controlled by disequilibrium kinetics, and Zr contents of granitic rocks can rarely be used to infer magma temperatures. However, Chappell et al. (2004) argued that the data on zircon saturation could be used to distinguish high-temperature granites from low-temperature granites in the Lachlan Orogen, Australia.

Samples with $M < 1.9$ have lower Ti-in-zircon temperatures than zircon saturation temperatures, as would be predicted if the zircon temperatures were recorded only in later formed crystals. However, similar temperatures are inferred from zircon rims and cores (Fig. 5). Furthermore, most samples with $M > 1.9$, have Ti-in-zircon temperature higher than zircon saturation temperature, contrary to these predictions. The high Ti-in-zircon temperatures for samples with $M > 1.9$ may simply reflect rock compositions that fall outside of the range of the experimental calibration. These questions are better pursued in studies of specific rock suites.

Ti-in-zircon temperatures from some of the Sierra Nevada granitoids ($M = 1.2$–1.8) and two of the four Yellowstone rhyolites (Mesa Falls, and Huckleberry Ridge Tuff A, $M = 1.3$; Bindeman and Valley 2001) record relatively high temperatures (695° to 950°C) with the highest values being equal to the zircon saturation temperature. The other rhyolites from Yellowstone (Lava Creek Tuff and Huckleberry Ridge Tuff C, $M = 1.3$–1.4; Bindeman and Valley 2001) have lower and more restricted Ti-in-zircon temperatures (625°–745°C) and the average Ti-in-zircon temperatures (645° and 710°C) are ~200°C below the expected zircon saturation temperature of their host rocks (Fig. 8). These Ti-in-zircon temperatures suggest that some rocks begin forming zircon at the saturation temperature and continue to crystallize zircon as the rock cools. Other samples appear to have formed zircon in a restricted range well below the saturation temperature. In either case most zircons from rocks with $M < 1.9$ are suggested to form at temperatures well below the saturation temperature.

Ti-in-zircon results from mafic rocks, discussed earlier, yield surprisingly low temperatures, lie outside the calibration for zircon saturation thermometry ($M > 1.9$, Fig. 8), and cannot be evaluated in terms of zircon saturation. It is significant that Hayden and Watson (2007) report generally lower values of a_{TiO_2} for mafic rocks if other parameters are constant, which suggests that Ti-in-zircon temperatures should requires a larger correction for reduced a_{TiO_2} for mafic compositions.

If the Ti-in-zircon temperatures of this study are correct, one explanation for values significantly below the estimated conditions of zircon saturation would be if the zircons formed from a late evolved hydrous melt with composition substantially different from the bulk rock. This hypothesis can be tested by petrographic observation. Zircons from rhyolite, both phenocrysts and xenocrysts with overgrowths, form in volcanic rocks that contain large amounts of glass, clearly attesting to incomplete crystallization and early growth of zircon (Bindeman and Valley 2001). Likewise, in plutonic rocks, zircons can crystallize well before the last melt. However, most of the zircons in this study (and, indeed, most zircons in other studies) were separated from crushed bulk rock samples for U-Pb geochronology and the petrologic context was lost. However, as a test of these ideas, zircons from the Temora-2 gabbroic diorite (Black et al. 2004) were analyzed as both mineral separates and in situ from a thin section of the same sample that was crushed to create the standard (L.P. Black pers. comm. 2005). Zircon inclusions in primary igneous hornblende record Ti-temperatures (746 ± 30°C) similar to interstitial zircons surrounded by plagioclase and quartz (729 ± 54°C), and to zircons separated from the rock (740 ± 76°C). More studies of zircons in thin section are needed, but at present, there is no textural evidence to support the hypothesis that low Ti-in-zircon temperatures uniformly correspond to highly evolved, late hydrous melts.

Possible non-equilibrium or non-Henry's Law behavior

In order to be an accurate geothermometer, Ti substitution in zircon must exhibit Henry's Law behavior and be an equilibrium process. Recent studies suggest that REE substitution into plagioclase (Bindeman and Davis 2000), apatite (Pan et al. 2003) and titanite (Prowatke and Klemme 2006) deviates from the behavior predicted by Henry's law, and that substitution of one trace element is enhanced by the presence of others. Furthermore, the trace element composition of zircon is generally quite variable within a single crystal, coupled substitutions are not well understood, and the effects of REE and other substitutions on Ti solid solution have not been evaluated. Possibly, Ti substitution is modified either by defects or by other trace element substitutions, which could explain patchy enrichment in Ti and REEs that has been observed in a zircon megacryst from kimberlite (Figs. 4a, 8b of Page et al. 2007a), and detailed element mapping, which shows Ti positively correlated to Y, Ce and P, especially in sector zones in zircon (Hofmann et al. 2007).

It is also possible that complex trace element zoning in igneous zircons reflects magma chamber processes.

Claiborne et al. (2006) demonstrated in the Spirit Mountain batholith, Nevada, that Hf (and U) are inversely correlated with Ti, and suggest large fluctuations in melt compositions and temperature. These authors concluded that the trace element zoning in zircon as well as whole-rock Zr/Hf should document repeated fractionation and thermal fluctuations. High Hf and low Zr/Hf in zircons may indicate growth from fractionated melt. A negative correlation of Hf and Ti is also seen for the Sierran zircons (Fig. 4). However, partitioning of a trace element between mineral and melt is not generally thought to be controlled by the concentration of other trace elements (e.g., Watson 1985), especially if the substitution is isovalent such as Ti for Si. Hayden and Watson (2007) show that Ti diffusion in melt is 2–3 times faster than Zr and thus that sluggish diffusion of Ti will not restrict equilibration of a growing zircon.

Lunar and high Ti terrestrial zircons

A relatively small number of terrestrial samples are reported that have Ti concentrations significantly higher than the averages in this study. One harzburgite xenolith from the Labait volcano, Tanzania, was found to contain a zircon with ~ 110 ppm Ti, the highest concentration yet reported in a terrestrial zircon (Watson et al. 2006), although when corrected for reduced a_{SiO_2} the Ti-temperature of this zircon is not consistent with independent thermometry (Ferry and Watson 2007). This Ti-rich zircon contrasts with the low average Ti concentration of mantle-derived zircon megacrysts from kimberlites of the Kaapvaal craton (13 ± 17 ppm, 114 analyses of 52 zircons from 7 kimberlite pipes; Page et al. 2007a). Other examples of high Ti zircons have been reported from metamorphic overgrowths in Neoproterozoic ultrahigh-temperature ($\sim 1,000°C$) granulites from the Anápolis-Itauçu Complex in central Brazil (34–52 ppm, Baldwin et al. 2007) and lower-crustal granulite xenoliths from the Lace kimberlite, Kaapvaal craton (78–97 ppm, Baldwin et al. 2007).

The only suite of zircons that is consistently high in Ti come from the Moon where magmas were hot and dry. Wopenka et al. (1996) analyzed a lunar zircon from a monzodiorite breccia and reported 59–161 ppm Ti, corresponding to Ti-in-zircon temperatures from 925° to 1,063°C. More recently, zircons from the KREEP-rich Apollo 14 landing site have yielded temperatures from 880° to 1,180°C (Taylor et al. 2007). While low fH$_2$O in lunar magmas is consistent with a higher temperature solidus, a possible effect of low fO$_2$ stabilizing Ti^{3+} or of unusual REE contents cannot presently be evaluated.

Jack Hills detrital zircons

The initial application of the Ti-in-zircon thermometer was to constrain the magmatic temperature and parent rock composition of >4.0 Ga detrital zircons from the Jack Hills, Western Australia. These are the oldest terrestrial materials, and the compositions of their original host rocks are unknown (Cavosie et al. 2007). Mojzsis et al. (2001) reported Jack Hills zircons with δ^{18}O from 8 to 15‰ VSMOW and asserted that these high values of δ^{18}O are igneous and thus that zircons formed from S-type granites. Watson and Harrison (2005) reported low Ti content for >4.0 Ga zircons, which yielded Ti-in-zircon temperatures of $696 \pm 66°C$, and concluded that the Jack Hills detrital zircons must have crystallized from wet granitic melts, indistinguishable from those produced in certain present-day geological environments. A larger Ti dataset and exclusion of samples with Ti-in-zircon temperatures above 750°C ($\sim 13\%$ the most Ti-rich zircons) reduced the estimate of temperature to $683 \pm 53°C$ (118 of 136 analyses) for crystallization of magmas that hosted the Jack Hill zircons (Watson and Harrison 2006; Harrison and Watson 2006; Harrison et al. 2007). Wet eutectic melting is proposed as the only geological process with sufficient reproducibility to explain the small variance and low temperatures of the majority of the detrital zircons. Zircons with more elevated temperatures (>750°C) are suggested to have a different provenance, perhaps higher-T tonalitic melts as proposed by Glikson (2006), Nutman (2006), and Valley et al. (2006).

Our Ti data from >4.0 Ga Jack Hills detrital zircons are consistent with the data reported by Watson and Harrison (2005, 2006) and Watson et al. (2006). The Ti-in-zircon temperatures for the Jack Hills detrital zircons of igneous origin range between 614° and 899°C with an average value of $717 \pm 108°C$ for 32 igneous zircons classified as type 1 of Cavosie et al. (2006). These temperatures are not correlated with zircon U-Pb age. The average drops to $699 \pm 66°C$ (27 zircons; or $692 \pm 65°C$, 41 analyses) if those with high Ti-in-zircon temperatures (>750°C) are excluded, as suggested by Watson and Harrison (2005, 2006) and Harrison et al. (2007). While the published data sets are quite similar, the interpretation of these data is not agreed upon.

In contrast to the conclusion that Jack Hills zircons came from S-type granites, we have interpreted the very high values of δ^{18}O = 8–15‰ as either altered or metamorphic (Peck et al. 2001; Cavosie et al. 2005; Valley et al. 2005, 2006) and recently, Trail et al. (2007) have accepted this conclusion. However, the expectation that zircons in rocks of mafic or intermediate composition will have Ti-in-zircon temperatures that are higher than and distinct

from the Jack Hills data has persisted. Our data do not support this conclusion.

The application of Ti content in zircon for identifying parent rock implicitly assumes that Ti-in-zircon temperatures are an accurate measure of actual magmatic conditions at the time of crystallization and that none of the issues relating to zircon thermometry, discussed above, are a significant problem. It is further assumed that the temperatures of zircon crystallization will be different for mafic vs. felsic rocks. A simple test of the conclusion that Ti content identifies Jack Hills zircons as granitic is to compare Ti in Jack Hills zircons to Ti in zircons obtained from a known parent rock. This approach removes any possible questions relating to thermometry.

Regardless of whether or not Ti content of zircon accurately reflects temperature of crystallization, the low Ti content of Jack Hills zircons can *only* be used to infer a granitic host if mafic zircons are consistently richer in Ti. Figure 9 shows that titanium-in-zircon temperatures and thus ppm Ti of Jack Hills zircons overlap those from a wide variety of igneous rocks (felsic to mafic) analyzed in this study. These histograms differ from Fig. 2 in that specific rock suites are shown. Some suites of mafic rocks contain higher Ti zircons, such as gabbros from the Mid-Atlantic ridge. However, other mafic rock suites, such as Precambrian anorthosites and gabbros from the Adirondack Mts, contain zircons with Ti-in-zircon temperatures that are

identical to the Jack Hills zircons. Furthermore, many suites of granitic rocks contain zircons with consistently lower Ti content than the Jack Hills, most notably the peraluminous granites from the Sierra Nevada batholith. The Ti-in-zircon temperatures of Jack Hills zircons can not be distinguished from many of the felsic, intermediate, and mafic rocks of this study, and thus Ti compositions do not identify the parent igneous rock of these detrital zircons (Valley et al. 2006).

Conclusions

Terrestrial zircons have Ti contents that are commonly less than ~ 20 ppm. On average, zircons from mafic igneous rocks have higher Ti concentrations than those from felsic rocks, but there is considerable overlap, and apparent Ti-in-zircon temperatures are lower than either zircon saturation temperatures for granitic rocks or predicted crystallization temperatures ($> \sim 15\%$ melt residue) for mafic rocks. In addition to temperature and TiO_2 activity, the activity of SiO_2 and pressure can affect the Ti content of zircon. However, these variables are not sufficient individually to explain the low temperatures reported here and a combination of additional confounding factors is suggested. Possible problems include: errors in calibration, a pressure effect, subsolidus resetting of Ti compositions, non-Henry's Law substitution of Ti in zircon, disequilibrium crystallization from melts, and growth of zircons in late melts with evolved hydrous composition. The results of this study do not directly implicate a single factor and it is likely that some combination of effects is important in controlling Ti-in-zircon.

Titanium concentrations in detrital zircons from the Jack Hills overlap those from both felsic and mafic rocks and are indistinguishable from several mafic suites, including gabbros and anorthosites. Furthermore, peraluminous granites yield significantly lower Ti-in-zircon temperatures than the Jack Hills suite. Thus, Ti-in-zircon thermometry alone is not sufficient to prove that the original parent rocks were water-saturated or "S-type" granites.

The titanium composition of zircon is highly sensitive to temperature and has been shown to correlate with other chemical indicators of magma evolution. As more understanding is gained of the controls on crystallization of zircon and zircon crystal chemistry, it is likely that this system will ultimately become an accurate and precise monitor of both igneous and metamorphic thermal history.
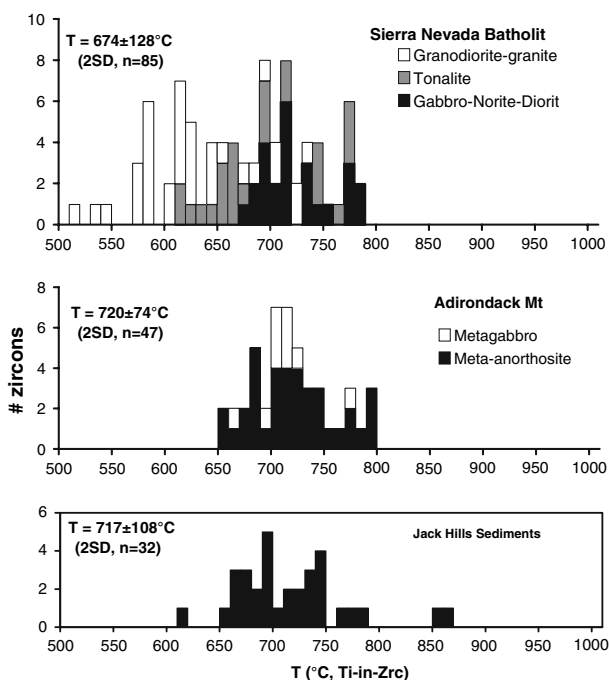

Fig. 9 Histograms of Ti-in-zircon temperatures estimated for zircons from the Sierra Nevada batholith, mafic rocks from the Adirondack Mountains (anorthosite, gabbro), and from Jack Hills metasediments

Appendix : Sample description

In total, 365 zircons from 45 igneous rock samples including localities in Nain, Adirondack Mountains, Sierra Nevada, Temora, and three well-known zircon standards were analyzed in this study. Detrital zircons from the Jack Hills and zircon xenocrysts from kimberlite were also studied.

Of seven anorthosite-leuconorite samples analyzed for titanium in zircon, four were collected from the Nain Anorthosite Complex, Labrador (Hamilton et al. 1994; Clechenko et al. 2003); three from the Woolen Mill locality, northeastern Marcy anorthosite massif, Adirondack Highlands, New York (McLelland et al. 2004). U-Pb ion microprobe ages of Nain anorthosite are 1,319–1,305 Ma (Hamilton et al. 1994). The Adirondack Mountains AMCG suite (anorthosite-mangerite-charnockite-granite) was intruded at $1,155 \pm 10$ Ma (McLelland et al. 2004), which establishes a coeval (but bimodal) origin for the AMCG suite. The Adirondack Mountains anorthosite was metamorphosed at granulite-facies conditions at about 1,050 Ma (McLelland et al. 2004).

Three samples of gabbro and fine-grained gabbroic dikes in serpentinite were collected from drill core (ODP Leg 153), located at the Mid-Atlantic Ridge near the Kane Transform (MARK area) (Cavosie et al. 2005a). Both $\delta^{18}O$ and REE distribution pattern indicate that zircons in serpentinite and gabbro are of magmatic origin.

Ten other gabbro samples were investigated from a variety of localities. Metagabbros include the Archean Pike Lake gabbro in Sturgeon Lake and the Kakagi Lake volcanics gabbro pegmatite, Wabigoon Subprovince (Davis et al. 1980, 1985; Davis and Edwards 1982; Davis and Trowell 1982; King et al. 1998); and Paleoproterozoic metagabbro sills at Prairie Creek and Bogus Jim Creek, Central Black Hills, Pennington County in South Dakota (Redden et al. 1990); Mesoproterozoic Woolen Mill metamorphosed ferrogabbro, northeastern Marcy massif, Adirondack Highlands, New York (McLelland et al. 2004); Neoproterozoic Palermo monzogabbro from the Serra do Mar Alkaline-Peralkaline Suite, Brazil (Valley et al. 2005); Cretaceous gabbro-norite in Western Sierra Nevada (Lackey 2005) and metagabbro-metadiorite from the Mount Stuart Batholith, Big Jim Mountain, Washington (Tabor et al. 1987). It is noteworthy that only the granulite-facies Woolen Mill metagabbro also yielded a metamorphic age, ~ 100 m.y. younger than the intrusive age, by ion microprobe U-Pb dating (McLelland et al. 2004), while the other metagabbros (or enclosed granophyre, see below) from both the Black Hills and Big Jim Mountain record only intrusive ages (Tabor et al. 1987; Redden et al. 1990).

Six other samples from mafic intrusions include a felsic segregation in gabbro from the Outer Eucrite Series in the Cullins and an alkaline segregation (feldspathic pegmatite) within the margin of the layered mafic/ultramafic complex, Isle of Skye, Scotland (Hamilton et al. 1998; Monani and Valley 2001); a trondhjemite pod within the Silurian Preston gabbro, an unmetamorphosed, stock-like intrusion in Griswold, New London County, Connecticut (Zartman and Naylor 1984); Mesoproterozoic greenish gray, medium-grained granophyre phases within a gabbro sill at the Crossport quarry, Eastport, Boundary County, Idaho (Zartman et al. 1982); and Paleoproterozoic coarse-grained granophyre in the upper part of the Nemo sill (i.e., 1,000-m-thick, gravity differentiated Blue Draw metagabbro), Black Hills, Lawrence County, South Dakota (Redden et al. 1990).

Eleven granitic samples were collected from the central part of the Sierra Nevada batholith, California (Lackey 2005; Lackey et al. 2005, 2006).

Five zircon samples were collected from volcanic rocks: basanite at Chantaburi, Thailand (Lee Silver pers. comm. 2000), and rhyolites from Yellowstone Plateau: Lava Creek Tuff, Mesa Falls Tuff and Huckleberry Ridge Tuff A and C (Bindeman and Valley 2001; Bindeman et al. 2001). One pegmatite sample was collected from the Central Adirondack Highlands, New York which yielded an ion microprobe U-Pb age of ~ 900 Ma (Valley et al. 2005).

Ti analyses were made on 42 detrital zircons obtained from quartzite and conglomerate from the Jack Hills, Western Australia with U/Pb ages >3,900 Ma. Additional information on these grains, including field locations, CL images, U/Pb and $\delta^{18}O$, REE data can be found in Cavosie et al. (2004, 2005b, 2006).

In addition, commonly used zircon standards for stable or radiogenic isotopes were assessed for Ti concentration and homogeneity. Zircon CZ3 is a detrital crystal from Sri Lanka (Pidgeon et al. 1994). Zircon 91500 is a megacryst from a titanite-bearing syenitic pegmatite in Ontario (Wiedenbeck et al. 2004). KIM-5 is a megacryst in kimberlite from the Kimberley Pool, South Africa (Valley et al. 1998; Valley 2003; Cavosie et al. 2005b). Temora-1 and Temora-2 are gabbroic diorites from the Lachlan Fold Belt, SE Australia (Black et al. 2004).

References

Asimow PD, Ghiorso MS (1998) Algorithmic modifications extending MELTS to calculate subsolidus phase relations. Am Mineral 83:1127–1132

Baker DR, Conte AM, Freda C, Ottolini L (2002) The effect of halogens on Zr diffusion and zircon dissolution in hydrous metaluminous granitic melts. Contrib Mineral Petrol 142:666–678

Baldwin JA, Brown M, Schmitz MD (2007) First application of titanium-in-zircon thermometry to ultrahigh-temperature metamorphism. Geology 35:295–298

Bea F, Montero PG, Gonzalez-Lodeiro F, Talavera C, Molina JF, Scarrow JH, Whitehouse MJ, Zinger T (2006) Zircon thermometry and U-Pb ion-microprobe dating of the gabbros and associated migmatites of the Variscan Toledo Anatectic Complex, Central Iberia. J Geol Soc London 163:847–855

Bindeman IN, Davis AM (2000) Trace element partitioning between plagioclase and melt: Investigation of dopant influence on partition behavior. Geochim Cosmochim Acta 64:2863–2878

Bindeman IN, Valley JW (2001) Low-δ^{18}O rhyolites from Yellowstone: magmatic evolution based on analyses of zircons and individual phenocrysts. J Petrol 42:1491–1517

Bindeman IN, Valley JW, Wooden JL, Persing HM (2001) Post-caldera volcanism: in situ measurement of U-Pb age and oxygen isotope ratio in Pleistocene zircons from Yellowstone caldera. Earth Planet Sci Lett 189:197–206

Black LP, Kamo SL, Allen CM, Davis DW, Aleinikoff JN, Valley JW, Mundil R, Campbell IH, Korsch RJ, Williams IS, Foudoulis C (2004) Improved $^{206}Pb/^{238}U$ microprobe geochronology by the monitoring of a trace-element-related matrix effect: SHRIMP, ID-TIMS, ELA-ICP-MS and oxygen isotope documentation for a series of zircon standards. Chem Geol 205:115–140

Bohlen SR, Essene EJ (1978) Igneous pyroxenes from metamorphosed anorthosite massifs. Contrib Mineral Petrol 65:433–442

Bohlen SR, Valley JW, Essene EJ (1985) Metamorphism in the Adirondacks: I, petrology, pressure and temperature. J Petrol 26:971–992

Carmichael ISE, Nichols J, Smith AL (1970) Silica activity in igneous rocks. Am Mineral 55:246–263

Carmichael ISE, Turner FJ, Verhoogen J (1974) Igneous petrology. McGraw Hill, New York, pp 1–739

Cavosie AJ, Wilde SA, Liu DY, Weiblen PW, Valley JW (2004) Internal zoning and U-Th-Pb chemistry of Jack Hills detrital zircons: a mineral record of early Archean to Mesoproterozoic (4348–1576 Ma) magmatism. Precambrian Res 135:251–279

Cavosie AJ, Kita NT, Valley JW (2005a) Magmatic δ^{18}O in zircons from gabbros and serpentinized peridotite at the Mid-Atlantic Ridge (ODP Leg 153). Eos Trans AGU, Abstr 86, OS33A-1453

Cavosie AJ, Valley JW, Wilde SA, EIMF (2005b) Magmatic δ^{18}O in 4400–3900 Ma detrital zircons: a record of the alteration and recycling of crust in the Early Archean. Earth Planet Sci Lett 235:663–681

Cavosie AJ, Valley JW, Wilde SA, EIMF (2006) Correlated microanalysis of zircon: trace element, δ^{18}O, and U–Th–Pb isotopic constraints on the igneous origin of complex >3900 Ma detrital grains. Geochim Cosmochim Acta 70:5601–5616

Cavosie AJ, Valley JW, Wilde SA (2007) The oldest terrestrial mineral record: a review of 4400 to 4000 Ma detrital zircons from the Jack Hills, Western Australia. In: van Kranendonk MJ, Smithies RH, Bennett VC (eds) Earth's oldest rocks. Developments Precambrian Geol 15:91–111

Chappell BW, White AJR, Williams IS, Wyborn D (2004) Low- and high-temperature granites. Trans R Soc Edinb Earth Sci 95:125–140

Cherniak DJ, Watson EB (2007) Ti diffusion in zircon. Chem Geol 242:470–483

Cherniak DJ, Hanchar JM, Watson EB (1997a) Diffusion of tetravalent cations in zircon. Contrib Mineral Petrol 127:383–390

Cherniak DJ, Hanchar JM, Watson EB (1997b) Rare-earth diffusion in zircon. Chem Geol 134:289–301

Claiborne LL, Miller CF, Walker BA, Wooden JL, Mazdab FK, Bea F (2006) Tracking magmatic processes through Zr/Hf ratios in rocks and Hf and Ti zoning in zircons: an example from the Spirit Mountain batholith, Nevada. Mineral Mag 70:517–543

Clechenko CC, Valley JW, Hamilton MA, Emslie RF (2003) Contamination of the Nain anorthosite: an oxygen isotope perspective. Geol Soc Am Ann Meet Abstr 35:630

Clemens JD (2003) S-type granitic magmas—petrogenetic issues, models and evidence. Earth Sci Rev 61:1–18

Coogan LA, Hinton RW (2006) Do the trace element compositions of detrital zircons require Hadean continental crust? Geology 34:633–636

Davis DW, Trowell NF (1982) U-Pb zircon ages from eastern Savant Lake-Crow Lake metavolcanic-metasedimentary belt, northwest Ontario. Can J Earth Sci 19:868–877

Davis DW, Edwards GR (1982) Zircon U-Pb ages from the Kakagi Lake area, Wabigoon Subprovince, northwest Ontario. Can J Earth Sci 19:1235–1245

Davis DW, Blackburn CE, Trowell NF, Edwards GR (1980) Geochronology of the Savant-Crow Lakes area, Western Wabigoon Subprovince, Districts of Kenora, Rainy River, and Thunder Bay. Ont Geol Surv Misc Paper 92:24–33

Davis DW, Krogh TE, Hinzer J, Nakamura E (1985) Zircon dating of polycyclic volcanism at Sturgeon Lake and implications for base metal mineralization. Econ Geol 80:1942–1952

Ferry JM, Watson EB (2007) New thermodynamic models and revised calibrations for the Ti-in-zircon and Zr-in-rutile thermometers. Contrib Mineral Petrol 154:429–437

Fournelle J (2008) The problem of secondary fluorescence in EPMA in the application of the Ti-in-zircon geothermometer and the utility of PENEPMA Monte Carlo program. Microsc Microanal (in press)

Fu B, Cavosie AJ, Clechenko CC, Fournelle J, Kita NT, Lackey JS, Page FZ, Wilde SA, Valley JW (2005) Ti-in-zircon thermometer: preliminary results. Eos Trans AGU, Abstr 86, V41F-1538

Ghiorso MS, Sack RO (1995) Chemical mass transfer in magmatic processes. IV. A revised and internally consistent thermodynamic model for the interpolation and extrapolation of liquid-solid equilibria in magmatic systems at elevated temperatures and pressures. Contrib Mineral Petrol 119:197–212

Glikson A (2006) Comment on "Zircon thermometer reveals minimum melting conditions on earliest Earth" I. Science 311:779a

Grimes CB, John BE, Kelemen PB, Mazdab FK, Wooden JL, Cheadle MJ, Hanghøj K, Schwartz JJ (2007) Trace element chemistry of zircons from oceanic crust: A method for distinguishing detrital zircon provenance. Geology 35:643–646

Hamilton MA, Emslie RF, Roddick JC (1994) Detailed emplacement chronology of basic magmas of the mid-Proterozoic Nain plutonic suite, Labrador: insights from U-Pb systematics in zircon and baddeleyite. In: Lanphere MA, Dalrymple GB, Turrin BD (eds) Abstracts of the eighth international conference on geochronology. Cosmochronology, and isotope geology. US Geol Surv Circ.vol 1107, p 124

Hamilton MA, Pearson DG, Thompson RN, Kelley SP, Emeleus CH (1998) Rapid eruption of Skye lavas inferred from precise U-Pb and Ar-Ar dating of the Rum and Cuillin plutonic complexes. Nature 394:260–263

Hanchar JM, Watson EB (2003) Zircon saturation thermometry. In: Hanchar JM, Hoskin PWO (eds) Zircon. Rev Mineral Geochem 53:89–112

Harrison TM, Schmidt AK (2007) High sensitivity mapping of Ti distributions in Hadean zircons. Earth Planet Sci Lett 261:9–18

Harrison TM, Aikman A, Holden P, Walker AM, McFarlane C, Rubatto D, Watson EB (2005) Testing the Ti-in-zircon thermometer. Eos Trans AGU, Abstr 86, V41F-1540

Harrison TM, Blichert-Toft J, Müller W, Albarede F, Holden P, Mojzsis SJ (2006) Response to comment on "Heterogeneous Hadean hafnium: evidence of continental crust at 4.4 to 4.5 Ga". Science 312:1139b

Harrison TM, Watson EB, Aikman AB (2007) Temperature spectra of zircon crystallization in plutonic rocks. Geology 35:635–638

Hayden LA, Watson EB (2007) Rutile saturation in hydrous siliceous melts and its bearing on Ti-thermometry of quartz and zircon. Earth Planet Sci Lett 258:561–568

Hinton RW, Upton BGJ (1991) The chemistry of Zircon—variations within and between large crystals from Syenite and Alkali Basalt Xenoliths. Geochim Cosmochim Acta 55:3287–3302

Hofmann AE, Cavosie AJ, Guan Y, Valley JW, Eiler JM (2007) Submicron-scale variations in Ti abundance in zircon. Geochim Cosmochim Acta 71(Suppl 1):A411

Holden P, Aikman A, Ireland TR, Heiss J (2005) Does Ti record the crystallization temperature of zircon? Eos Trans AGU, Abstr 86, V41F-1539

King EM, Valley JW, Davis DW, Edwards GR (1998) Oxygen isotope ratios of Archean plutonic zircons from granite-greenstone belts of the Superior Province: indicator of magmatic source. Precambrian Res 92:365–387

Lackey JS (2005) The magmatic and alteration history of the Sierra Nevada Batholith as recorded by oxygen isotope ratios of Zircon, Titanite, Garnet, and Quartz. University of Wisconsin, Madison, Unpublished PhD Dissertation, pp 1–344

Lackey JS, Valley JW, Saleeby JB (2005) Supracrustal input to magmas in the deep crust of Sierra Nevada batholith: evidence from high-δ^{18}O zircon. Earth Planet Sci Lett 235:315–330

Lackey JS, Valley JW, Hinke HJ (2006) Deciphering the source and contamination history of peraluminous magmas using δ^{18}O of accessory minerals: examples from garnet-bearing granitoids of the Sierra Nevada batholith. Contrib Mineral Petrol 151:20–44

Llovet X, Salvat F (2006) PENEPMA, A Monte Carlo Code for the simulation of X-ray emission spectra using PENELOPE, Madison WI Workshop Manual (unpublished)

Maas R, Kinny PD, Williams IS, Froude DO, Compston W (1992) The Earth's oldest known crust: a geochronological and geochemical study of 3900–4200 Ma old detrital zircons from Mt. Narryer and Jack Hills, Western Australia. Geochim Cosmochim Acta 56:1281–1300

McLelland JM, Bickford ME, Hill BM, Clechenko CC, Valley JW, Hamilton MA (2004) Direct dating of Adirondack massif anorthosite by U-Pb SHRIMP analysis of igneous zircon: implications for AMCG complexes. Geol Soc Am Bull 116:1299–1317

Monani S, Valley JW (2001) Oxygen isotope ratios of zircon: magma genesis of low δ^{18}O granites from the British Tertiary Igneous Province, western Scotland. Earth Planet Sci Lett 184:377–392

Nutman A (2006) Comment on "Zircon thermometer reveals minimum melting conditions on earliest Earth" II. Science 311:779b

Page FZ, Fu B, Kita NT, Fournelle J, Spicuzza MJ, Schulze DJ, Viljoen F, Basei MAS, Valley JW (2007a) Zircons from kimberlite: new insights from oxygen isotopes, trace element, and Ti in zircon thermometry. Geochim Cosmochim Acta 71:3887–3903

Page FZ, Ushikubo T, Kita NT, Riciputi LR, Valley JW (2007b) High-precision oxygen isotope analysis of picogram samples reveals 2 μm gradients and slow diffusion in zircon. Am Mineral 92:1772–1775

Pan Y, Dong P, Chen N (2003) Non-Henry's Law behavior of REE partitioning between fluorapatite and CaF2-rich melts: Controls of intrinsic vacancies and implications for natural apatites. Geochim Cosmochim Acta 67:1889–1900

Peck WH, Valley JW, Wilde SA, Graham CM (2001) Oxygen isotope ratios and rare earth elements in 3.3 to 4.4 Ga zircons: ion microprobe evidence for high δ^{18}O continental crust and oceans in the Early Archean. Geochim Cosmochim Acta 65:4215–4229

Peck WH, Valley JW, Graham CM (2003) Slow oxygen diffusion rates in igneous zircons from metamorphic rocks. Am Mineral 88:1003–1014

Pidgeon RT, Furfaro D, Kennedy AK, Nemchin AA, Van Bronswijk W (1994) Calibration of zircon standards for the Curtin SHRIMP II. In: Abstracts 8th international conference on geochronology, cosmochronology, and isotope geology, US Geol Surv Circ. vol 1107, p 251

Prowatke S, Klemme S (2006) Rare earth element partitioning between titanite and silicate melts: Henry's law revisited. Geochim Cosmochim Acta 70:4997–5012

Redden JA, Peterman ZE, Zartman RE, DeWitt E (1990) U-Th-Pb geochronology and preliminary interpretation of Precambrian tectonic events in the Black Hills South Dakota. In: Lewry JF, Stauffer MR (eds) The early Proterozoic Trans-Hudson Orogen of North America. Geol Assoc Can Spec Pap 37, pp 229–251

Ryerson FJ, Watson EB (1987) Rutile saturation in magmas: implications for Ti-Nb-Ta depletion in island-arc basalts. Earth Planet Sci Lett 86:225–239

Schmitt AK, Vazquez JA (2006) Alteration and remelting of nascent oceanic crust during continental rupture: evidence from zircon geochemistry of rhyolites and xenoliths from the Salton Trough, California. Earth Planet Sci Lett 252:260–274

Tabor RW, Frizzell VA Jr, Whetten JT, Waitt RB, Swanson DA, Byerly GR, Booth DB, Hetherington MJ, Zartman RE (1987) Geologic map of the Chelan 30-minute by 60-minute quadrangle, Washington. US Geol Surv Misc Invest Ser Map I-1661, pp 1–33

Taylor DJ, McKeegan KD, Harrison TM, McCulloch M (2007) ^{176}Lu-^{176}Hf in lunar zircons: Identification of an early enriched reservoir on the moon. Lunar Planet Sci XXXVIII:2130

Trail D, Mojzsis SJ, Harrison TM, Schmitt AK, Watson EB, Young ED (2007) Constraints on Hadean zircon protoliths from oxygen isotopes, Ti-thermometry, and rare earth elements. Geochem Geophys Geosys 8:Q06014, doi:10.1029/2006GC001449

Urusov VS, Dudnikova VB (1998) The trace-component trapping effect: experimental evidence, theoretical interpretation, and geochemical applications. Geochim Cosmochim Acta 62:1233–1240

Ushikubo T, Kita NT, Cavosie AJ, Wilde SA, Rudnick RL, Valley JW (2008) Lithium in Jack Hills zircons: evidence for extreme weathering of Earth's earliest crust. Earth Planet Sci Lett (in review)

Valley JW (2003) Oxygen isotopes in zircon. In: Hanchar JM, Hoskin PWO (eds) Zircon. Rev Mineral Geochem 53:343–385

Valley JW, Kinny PD, Schulze DJ, Spicuzza MJ (1998) Zircon megacrysts from kimberlite: oxygen isotope heterogeneity among mantle melts. Contrib Mineral Petrol 133:1–11

Valley JW, Lackey JS, Cavosie AJ, Clechenko CC, Spicuzza MJ, Basei MAS, Bindeman IN, Ferreira VP, Sial AN, King EM, Peck WH, Sinha AK, Wei CS (2005) 4.4 billion years of crustal maturation: oxygen isotope ratios of magmatic zircon. Contrib Mineral and Petrol 150:561–580

Valley JW, Cavosie AJ, Fu B, Peck WH, Wilde SA (2006) Comment on "Heterogeneous Hadean Hafnium: Evidence of Continental Growth at 4.4 to 4.5 Ga". Science 312:1139a

Wark DA, Watson EB (2006) TitaniQ: a titanium-in-quartz geothermometer. Contrib Mineral Petrol 152:743–754

Watson EB (1985) Henry's law behavior in simple systems and in magmas: criteria for discerning concentration-dependent partition coefficients in nature. Geochim Cosmochim Acta 49:917–923

Watson EB, Harrison TM (1983) Zircon saturation revisited: temperature and composition effects in a variety of crustal magma types. Earth Planet Sci Lett 64:295–304

Watson EB, Harrison TM (2005) Zircon thermometer reveals minimum melting conditions on earliest Earth. Science 308:841–844

Watson EB, Harrison TM (2006) Response to comments on "Zircon thermometer reveals minimum melting conditions on earliest Earth". Science 311:779c

Watson EB, Wark DA, Thomas JB (2006) Crystallization thermometers for zircon and rutile. Contrib Mineral Petrol 151:413–433

Wiedenbeck M, Hanchar JM, Peck WH, Sylvester P, Valley J, Whitehouse M, Kronz A, Morishita Y, Nasdala L (2004) Further characterization of the 91500 zircon crystal. Geostand Geoanal Res 28:9–39

Wilde SA, Valley JW, Peck WH, Graham CM (2001) Evidence from detrital zircons for the existence of continental crust and oceans on the Earth 4.4 Gyr ago. Nature 409:175–178

Wopenka B, Jolliff BL, Zinner E, Kremser DT (1996) Trace element zoning and incipient metamictization in a lunar zircon: application of three microprobe techniques. Am Mineral 81:902–912

Zartman RE, Naylor RS (1984) Structural implications of some radiometric ages of igneous rocks in southeastern New England. Geol Soc Am Bull 95:522–539

Zartman RE, Peterman ZE, Obradovich JD, Gallego MD, Bishop DT (1982) Age of the Crossport C sill near Eastport, Idaho. In: Reid RR, Williams GA (eds) Soc Econ Geol Coeur d'Alene Field Conf Idaho-1977. Idaho Bureau Mines Geol Bull 24:61–69